

Uplink-downlink resource optimization for provisioning 5G application considering SUI fading channel models

Vanita Kaba, Rajendra R. Patil

Department of Electronics and Communication, GSSS Institute of Engineering and Technology for Women Mysore,
Affiliated to Visvesvaraya Technological University, Belagavi, India

Article Info

Article history:

Received Dec 5, 2023

Revised Dec 25, 2023

Accepted Jan 6, 2024

Keywords:

Bit error rate

Effective resource allocation

Power domain

Signal to noise ratio

Zadoff chiu

ABSTRACT

Recently, superposition coding (SC), Stanford University Interim (SUI) fading channel, user clustering, successive interference cancellation (SIC) mechanism has been incorporated into the power allocation design for attaining good performance. Nonetheless, the existing model works with cluster size up to 4 user per cluster and induce higher control channel overhead. In addressing this paper introduce an effective resource allocation (ERA) design for power domain non-orthogonal multiple access (PD-NOMA) system. The ERA, first employ Zadoff Chu (ZC) coding, then power is allocated according to the distance considering 5 user per cluster. Finally, multi-level SIC is done at the receiver end. The ERA performance is studied by varying signal-to-noise ratio (SNR) in terms of bit error rate (BER) considering a maximum of five users per cluster. Further, the ERA performance in terms of BER is tested under different scenario defined in SUI propagation scenario such as higher pathloss, moderate path loss, and low path loss. The throughput performance under varied density and speed is also studied; the ERA achieves much better performance in terms of ERA, SNR and throughput than standard multi-user downlink resource allocation (MUDRA) model.

This is an open access article under the [CC BY-SA](https://creativecommons.org/licenses/by-sa/4.0/) license.



Corresponding Author:

Vanita Kaba

Department of Electronics and Communication, GSSS Institute of Engineering and Technology for Women Mysore, Affiliated to Visvesvaraya Technological University

Belagavi, India

Email: vbkaba@gmail.com

1. INTRODUCTION

The escalating need for enhanced speed of data driven by the emergence of network protocols like fifth generation (5G) and sixth generation (6G) applications [1], [2], encompassing domains that include the internet of things (IoTs), video conferencing, vehicular communication, wearable devices and satellite communication, has undergone significant advancements. The proliferation of wireless networks has led to the integration of autonomous devices, including self-driving automobiles, intelligent houses, sophisticated cognitive technology, and various other applications. The observed outcome of this phenomenon is a notable rise in the quantity of consumers within the network cell, consequently transforming it into an ultra-dense cells [2]. The current resources available, including orthogonal-multiple-access (OMA) methods, are constrained by their orthogonalization, resulting in limitations on the total amount of users they can accommodate. Consequently, these methods are inadequate for addressing the demands of contemporary wireless communication. In order to ensure the fulfillment of these requirements, various access methods have been developed in prior works [3], [4]. These methods enable multiple users to efficiently utilize the available resources and effectively serve to overcrowded systems. Moreover, several noteworthy methods are

being recognized in the realm of 5G networks. These include non-orthogonal multiple access (NOMA) [3], sparse-code-multiple-access (SCMA) [5], [6], low-density spreading multiple-access (LDSMA) [7], pattern-division multiple-access (PDMA) [8], massive multiple-input and multiple-output (massive MIMO) [9], cooperative-communication [10], [11], and other similar approaches. Every one of the aforementioned 5G methods possesses distinct characteristics and is categorized according to various factors such as quality-of-service (QoS), user-fairness, spectrum efficiency, minimal latency, and level of freedom. NOMA, an innovative technique for 5G networks, has been proposed as a means to alleviate the limitations imposed by orthogonality in both time and frequency domains, particularly in scenarios where cells are in close proximity to each other [12], [13].

The investigation of NOMA methods with superposition-coding at the point of transmission and successive-interference-cancellation (SIC) at the receiving ends is currently being conducted to meet the requirements of users in 5G wireless networks. According to the research conducted, NOMA has been found to provide several advantages including minimal latency, greater transfer rates, improved connectivity, and enhanced user-fairness [14]. In contrast to the orthogonal multiple access (OMA) strategies [15], NOMA enables simultaneous and concurrent service provision to users operating on identical frequency and time resources. In the past few years, there have been a presentation of two distinct types of NOMA techniques, namely power-domain NOMA (PD-NOMA) and code-domain NOMA (CD-NOMA) [16], [17].

In the context of PD-NOMA [5], it is observed that distinct power-levels (PLs) are allocated to user-signals prior to the implementation of superposition-coding at the transmitter. The assignment of PLs is determined by considering the diverse distances along with channel-gains experienced by individual users. In the pursuit of attaining user-fairness in PD-NOMA systems, a notable approach involves the allocation of higher PLs for the signals of users who are situated greater distances away from the transmitter. The PLs assigned to users in proximity to the transmitter are comparatively lower, and this pattern continues for users located further away. Mahmood *et al.* [18] introduced user clustering up to 4 user per-cluster for power allocation and interference is addressed through multi-level SIC. However, the user density is expected to increase in 5G network, which prerequisite the power allocation design to accommodate higher cluster size. This motivates the research work develop 5 user per cluster for PD-NOMA system. Further, the existing induce higher delay and control channel overhead due to usage of superposition coding (SC); In reducing delay and control channel overhead the Zadoff Chu (ZC) coding is used. Finally, multi-level SIC similar to [18] is performed. The significance of the research work are as follows:

- The ERA uses ZC to improve the speed of encoding and reduce control channel overhead.
- ERA allow user clustering up to 5 user per cluster and multi-level SIC in PD-NOMA system.
- The ERA work well under different path loss scenario i.e., high, moderate, and low path loss scenario.
- The ERA attain better throughput and BER performance in comparison with existing multi-user downlink resource allocation (MUDRA) model.

The manuscript is organized as follows. The section 2, studies various existing power allocation and SIC methodologies for PD-NOMA system and highlight the benefits and limitation of existing methodologies. In section 3, the proposed methodology of effective resource allocation (ERA) design is presented. In section 4, the outcome obtained using ERA over MRUDA is provided. The last section provide the summary of the work and its enhancement over state-of-art power allocation design and future scope of the work is highlighted.

2. LITERATURE SURVEY

This section presents survey of various technique of channel access mechanism in next-generation wireless network leveraging OMA and PD-NOMA system and highlight its significance and limitation of the current approaches. According to [19], PD-NOMA improves user-fairness and spectrum efficacy, making it desirable. Moreover, their assumption is that the NOMA's practical execution is hindered by radio-frequency limitations like power-amplification (PA) nonlinearity (PAN). This work examined how PAN affects PD-NOMA identification and suggested a random-fourier-feature (RFF)-based approach. The suggested RFF based approach yielded findings that were remarkably nearly identical to the perfect situation and substantially enhanced BER performance, according to computer simulations run under various PAN variations.

Fu *et al.* [5], suggested a PD-NOMA along with sparse-code multiple-access (SCMA) uplink network to provide vast user connection. The receiver itself decodes overlaid signals using SIC and recurrent SCMA detection. By examining extrinsic-information transfer (EXIT) graphs, the rate of code transfer for error-correcting channel codes were optimized to balance network converging characteristics and spectral efficacy. The optimizing approach enhanced the spectral efficacy and BER. Luo *et al.* [6], compared the error rates of PD-NOMA and SCMA. With a standard PD-NOMA network [20], [21], SIC at the receiving end may propagate errors. Hence, SCMA uses transmission of messages decoding. By optimizing power-allocation with pairwise-error likelihood and decoding using extended spherical decoder is the ideal way to

maximize PD-NOMA error-free efficiency. Lastly, this work concluded that channel estimate error affects GSD-based PD-NOMA, SIC, rayleigh-fading, and SCMA complicates multi-user detection techniques.

The primary objective of [22], was to explore and analyze the possible abilities of power-domain PD-NOMA frameworks [23]. The outcomes of simulation-based modeling were presented to assess the efficacy of PD-NOMA frameworks during the uplink. This situation holds particular importance for IoTs networks, making it an intriguing area of study. In order to facilitate uplink video interactions [24], suggested a recursive codebook allocation that spans both the application and physical-layers. The channel-specific state data of the physical-layer determines the codebook allocation, and users interchange codebooks to reduce the video mean-square-error (MSE) and raise the average peak-signal-to-noise-ratio (PSNR). Additionally, this work suggested a deep-neural-network (DNN) method to simplify calculation. Next, a post-processing procedure was used to DNN outputs to meet codebook assigned requirements.

The study [11] optimized allocation of power using foliage depth, SNR, and distance constraints. The fuzzy-inference technique assigned optimum power factors (PFs) to users near 5G base-station (BS). The network used collaborative relays near the user's location to reduce signal loss and routing loss towards the faraway user. In 5G PD-NOMA, feasible micro-cells used different ways to improve system efficiency. In particular, the transmitting device used SC to effectively distribute energy and broadcast numerous signals. At the near-user side, SIC reduced overlaid interference with signals. Lastly, the far-user receiver used maximal-ratio combination (MRC) to optimize signal combination and reliability. These methods made the downlink PD-NOMA network more efficient and reliable in a 5G micro-cell scenario. Considering varied SNR conditions, easy-to-use and collaborative relaying PD-NOMA systems were examined for BER. Studies show that Collaborative PD-NOMA outperforms basic PD-NOMA. The suggested approach ensured equitable user-fairness in PD-NOMA systems through collaborative interaction, thereby improving system efficiency.

5G BS and registered users communicate using a revolutionary low-complex short code-based method [25]. This secures PD-NOMA from anonymous users and interceptors [26]. Yue *et al.* [26], they developed a 3-step user-clustering approach to boost efficiency by choosing the most efficient cluster from all available clusters. Clustering reduces PD-NOMA failure likelihood. A multi-user decoding and forwarding collaborative relaying method using PD-NOMA was also presented called as Cop-PD-NOMA to expand 5G BS connectivity, In the multi-user Cop-PD-NOMA, powerful users (close to users) transmitted help to weaker users (away users) by means of forward and decode (F&D). A secure PD-NOMA network and the best user clustering method were achieved throughout validation. Multi-user collaboration excels over single-user collaboration in Cop-PD-NOMA transmission based on BER evaluations. The efficiency of multi-user downlink PD-NOMA was assessed in suburban settings, specifically considering the effects of SUI channel fading [18]. The allocation of PLs to baseline controlled user communication with phase changes was determined based upon the location of the users from the BS, prior to the implementation of Superposition-coding [27]. At the receiver ends, a multi-level SIC technique was employed. The objective of this study was to analyze the efficiency of BER in relation to SNR for a maximum of 4 users for each cluster. The comparison was conducted across various SUI systems that match to various suburban environments, each characterized by differing vegetation density values. The evaluation also includes an assessment of the maximum number of users for each cluster which can be facilitated under benchmark BER and SNR values. However, the traditional model induces control channel overhead and supports user per cluster size of 2 to 4. In addressing the next section present methodology that address control channel, reduce delay and support 5 user per cluster for power allocation in PD-NOMA system.

3. RESEARCH METHOD

Uplink-downlink resource optimization for 5G applications refers to the efficient allocation and management of communication resources in both the uplink and downlink directions of wireless communication networks. This optimization is essential for delivering the high-performance and low-latency requirements of diverse 5G applications, which include a wide range of services such as enhanced mobile broadband (eMBB), massive machine-type communication (mMTC), and ultra-reliable low-latency communication (URLLC). This section outlines the approach employed in our study to optimize uplink-downlink resource-optimization for 5G applications, with a specific focus on incorporating SUI fading-channel models.

3.1. System model

The schematic diagram presented in Figure 1 illustrates a single-input single-output (SISO) downlink PD-NOMA system. In this setup, a BS is responsible for sending a combination of signals to a group of N user-equipment (UEs). The signal of every user is subjected to base-band modulation employing binary-phase shift-keying (BPSK) and subsequently assigned a power-factor (PF) that is determined by its distance from the BS. The process of superposition-coding is executed at the BS in order to generate the

combination of signals. The combined signal undergoes transmission by carrying out a selective fading-channel known as the SUI channel, while being subjected to the presence of additive white gaussian noise (AWGN). The utilization of a root-raised cosine (RRC) filtering is a common practice in each of the transmitting and receiving stages of a communication system. This filter serves the purpose of pulse-shaping, which is essential for the mitigation of inter-symbol interference (ISI). The signal received is subjected to decoding processes by individual receivers, employing distinct stages of SIC techniques. Figure 2 shows the block diagram of all the steps which have been considered in the proposed model for transmitting signal from sender Tx to the receiver Rx.

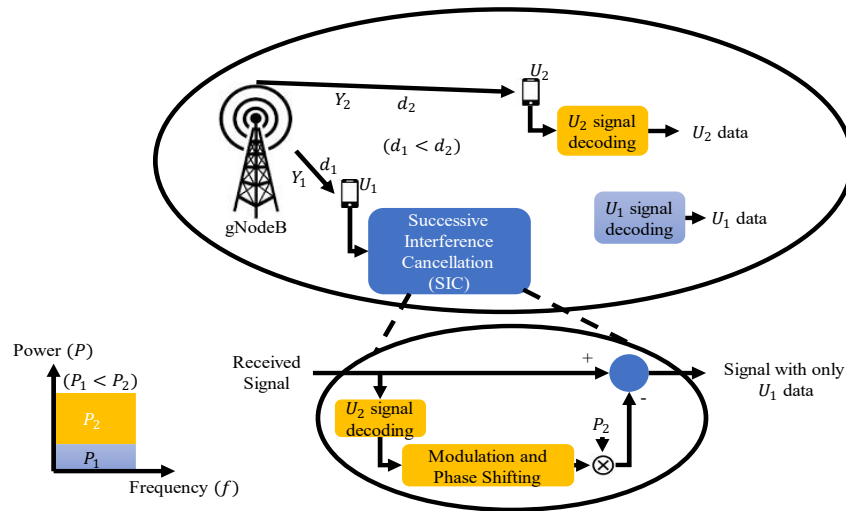


Figure 1. SISO downlink PD-NOMA system (U1 is near-user and U2 is far-user)

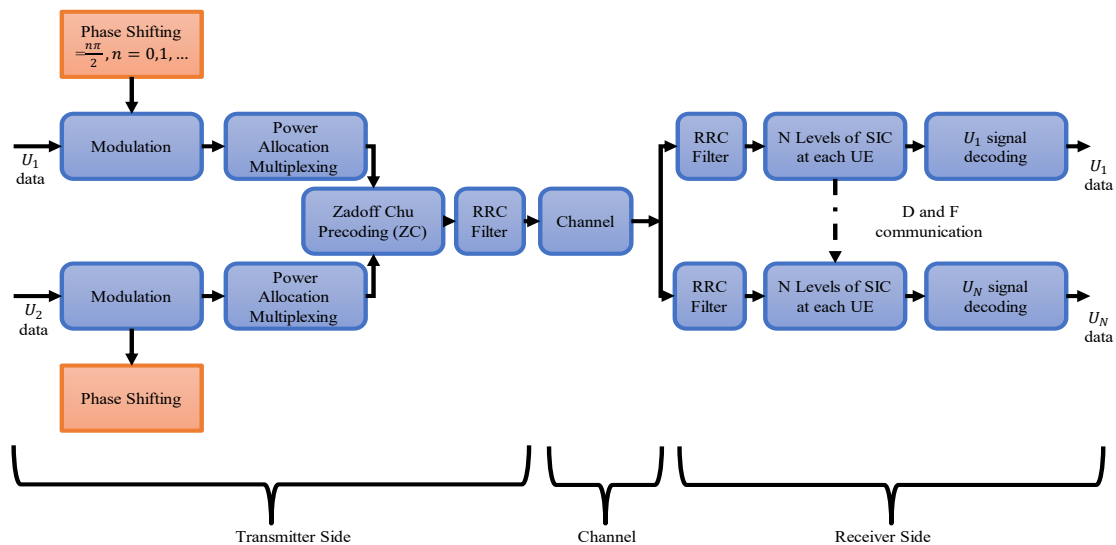


Figure 2. Block diagram for all the steps taken between Tx and Rx in the proposed PD-NOMA system

The signal generated by the users within a cluster is subjected to modulation and allocated specific PF. This ensures that the combined signal is transmitted through the BS and is expressed using (1). In this study, we consider the variable m which takes values starting from 1 and incrementing by 1, i.e., $m = 1, 2, 3, \dots M$. The variable M represents the total count of clusters. Meanwhile, the variable k takes values starting from 1 and incrementing by 1 until a certain condition is met, i.e., $k = 1, 2, 3, \dots N$. The variable N represents the total count of users within a given cluster. The variable $s_m, k(t)$ denotes the communication signal associated with the k^{th} user within the m^{th} cluster. Additionally, p_k represents the allocated PF for the specific user. In the pursuit of achieving user-fairness in PD-NOMA systems, a strategy is employed wherein lower PLs are assigned

to UEs that are in close proximity with the BS, while higher PLs are assigned to UEs that are situated at greater distances away from the BS. This allocation pattern is then extended to subsequent UEs in a similar manner.

$$c_m(t) = \sum_{k=1}^N \sqrt{p_k} s_m, k(t) \tag{1}$$

The total transmit power is defined through parameter p_b and the total power allocated to each user is equal or less than the total transmitted power, which is represented using (2). Each PL is allocated in such a way that the total of all PFs equals one. i.e., using (3). The power-allocation is determined by considering the channel-gain and distance from BS of every user. The channel-gains of users $r_1, r_2, r_3,$ and r_4 are arranged in the following order: $h_1 > h_2 > h_3 > h_4$, as depicted in Figure 3. The PFs exhibit a hierarchical relationship, with p_1 being the lowest and p_4 being the highest, based on the current channel requirements.

$$p_1 + p_2 + p_3 + p_4 \leq p_b \tag{2}$$

$$\sum_{k=1}^N p_k = 1 \tag{3}$$

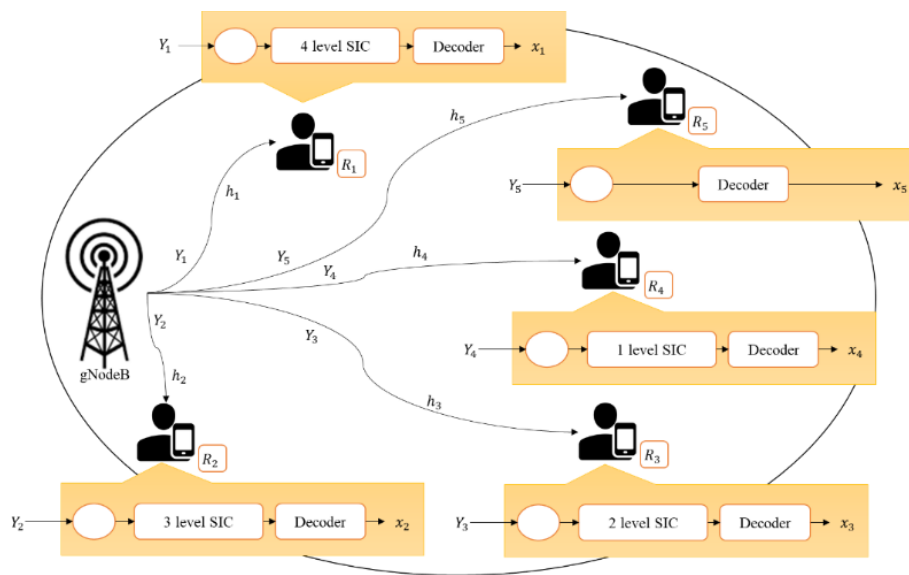


Figure 3. Block diagram of multi-user downlink PD-NOMA with the channel gains order $h_1 > h_2 > h_3 > h_4$

3.2. Mitigating interference

This work uses phase-shift (PS) when modulating user signals to get across the significant interference caused by several users within the cluster. People using the service are subject to an overall PS of $\frac{\pi}{2}$ as presented in (4). In this study, the variable n is defined as ranging from 0 to $N - 1$, where N represents the overall total of users for every cluster. Within a cluster consisting of 4 users, denoted as $UE_1, UE_2, UE_3,$ and UE_4 , each user’s signal exhibits a distinct PS. Specifically, UE_1 encounters a PS of 0 radians, UE_2 encounters a PS of $\frac{\pi}{2}$ radians, UE_3 encounters a PS of π radians, and UE_4 encounters a PS of $\frac{3\pi}{2}$ radians. The distribution of PLs is determined by considering the distance of every user, as discussed in [16], i.e., using (5).

$$Phase\ Shift\ (PS) = \pm \frac{n\pi}{2} \quad n = 0,1,2 \dots \tag{4}$$

$$p'_i = \frac{d_i}{d_1} \quad i = 1,2 \dots N \tag{5}$$

The total PF, denoted as p'_i , is a crucial parameter in the context of wireless communication systems. It is worth noting that d_i represents the total distance of the i th user to the BS. In this particular scenario, the value of d_1 is set to 200 m, which is a commonly observed radius for BS coverage in 5G networks. The PFs are adjusted within the range of 0 to 1, in accordance with (6). Next, the RRC-filter (RRCF) is applied to every

cluster’s combined signal $c_m(t)$, ensuring (7). The signal that is transmitted for a cluster is denoted as $x_m(t)$, whereas the response of the RRCF is represented by $g(t)$. The signals from every cluster are superimposed using (8).

$$p_i = \frac{p'_i}{\sum_{i=1}^N p'_i} \quad i = 1, 2 \dots N \tag{6}$$

$$x_m(t) = \sum_j c_m(t)g(t - kT) \tag{7}$$

$$x(t) = \sum_{m=1}^M x_m(t) \tag{8}$$

The combined signal $x(t)$ undergoes transmission using the SUI channel-model. The signal received by every UE encounters significant changes in signal strength due to environmental factors which is determined using (9). The variable α_k represents the path-gain, while n_k represents the AWGN associated with every k th user. Every UE gets the combined signal, that is then routed by means of RRCF for pulse structuring in order to minimize ISI. The signal is then decoded by implementing various levels of SIC at every receiver, as depicted in Figure 4. The resulting decoded signal is denoted as (10). The value of l ranges from 0 for the longest UE to $N - 1$ for the closest UE in (10).

$$y_k(t) = \alpha_k \cdot x(t) + n_k(t) \quad k = 1, 2, 3 \dots \tag{9}$$

$$\hat{x}_k(t) = y_k(t) - \sum_l x_l(t) \tag{10}$$

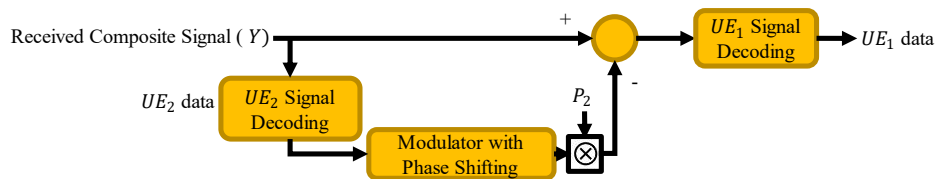


Figure 4. SIC at the Rx of UE1 in two users per cluster PD-NOMA system

3.3. Multi-user signal interference cancellation technique

SIC is an essential component of NOMA systems, as it serves the purpose of mitigating the negative effects caused by interference signals originating from concurrent users. The combined signal, which encompasses all individual user signals, is received by every receiver. In a cluster consisting of N users, it is observed that the UE closest to the BS engages in $N-1$ levels of SIC. Similarly, the UE that is next closest towards the BS engages in $N-2$ levels of SIC, and this pattern continues for the remaining UE s in the cluster. The user located at the longest distance is able to successfully decode the signal using only the combined signal, without the need for SIC techniques. To ensure equitable treatment of users, i.e., user-fairness, the allocation of the total transmit power is determined based upon the individual channel-coefficients and user-distance. In accordance with established protocols, the decoding process prioritizes signals using the highest PL. Subsequently, signals with progressively lower PLs are decoded in the order of decreasing PL.

In a conventional two-user PD-NOMA framework, the presence of two users, namely UE_1 (cell-center user) and UE_2 (cell-edge user), necessitates the implementation of SIC technique. This technique involves the utilization of UE_1 , which is in close proximity to the BS, to mitigate any disruption resulting from the signal transmitted by UE_2 . By employing SIC, the disruption induced by UE_2 signal can be effectively canceled, thereby enhancing the overall system performance. At the receiving end of UE_1 , the demodulation and decoding process prioritizes the signal from UE_2 through a higher PL. The signal undergoes modulation once more, followed by multiplication with its unique PF, and subsequently subtraction from the combined signal, thereby facilitating the decoding of the UE_1 signal. The aforementioned observation is visually depicted in Figure 4.

In the context of a PD-NOMA structure with a cluster configuration consisting of four users, it is observed that each UE is required to decode signals with relatively higher PLs, as depicted in Figure 5. The user denoted as UE_4 is able to extract its signal straight from the combined signal, thereby achieving the maximum distance of transmission. In the context of UE communication systems, it has been observed that UE_3 , which is ranked as the next most distant user, engages in a process known as SIC. This process involves several steps, beginning by performing the decoding of the signal transmitted by UE_4 . Once the signal from

UE_4 has been successfully decoded, UE_3 proceeds to modulate it. This modulation process involves modifying the characteristics of UE_4 signal in order to suit the specific requirements of UE_3 . Additionally, UE_3 multiplies the modulated signal using a PF, which allows for further adjustments to the signal's PL.

Finally, UE_3 subtracts the resulting modulated and power-adjusted signal through the combined signal it receives. This subtraction step is crucial in mitigating interference and enhancing the overall quality of the received signal. Consequently, the combined signal is processed, along with the UE_3 signal identified as the dominant signal in terms of power, and subsequently decoded. The UE_2 receiver engages in SIC techniques to process the data signals from UE_4 and UE_3 , while UE_1 employs SIC for obtaining its very own signals from UE_4 , UE_3 , and UE_2 signals, respectively.

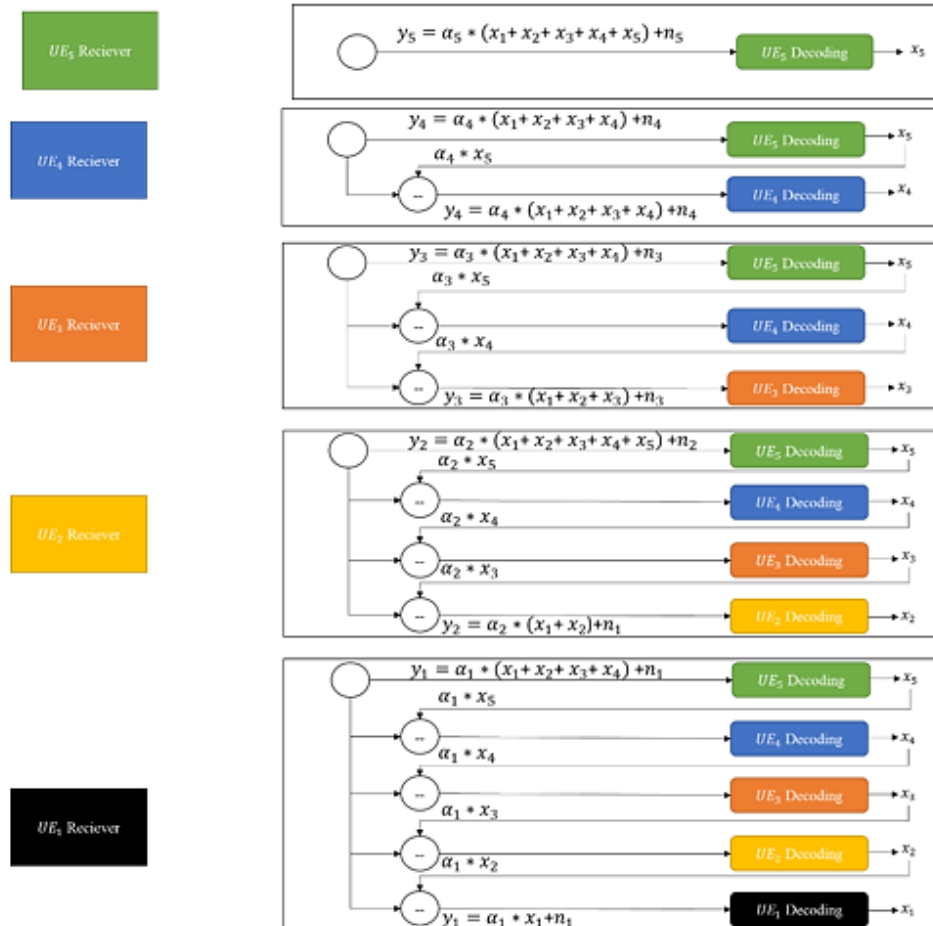


Figure 5. Block diagram for all the steps taken between Tx and Rx in the proposed ERA in PD-NOMA system

3.4. SUI channel modelling

The SUI channel model was introduced in [28] and is further extended for sub-urban and heavy-vegetation with SUI propagation model in [29]; further, according to environment condition it is further divided into three scenarios as defined below. The scenario 1, defines a hilly area with very good amount to heavy tree densities; the environment exhibits very high path loss. The scenario 2, defines a hilly climatic condition with vast vegetation at the terrain level; the environment exhibits moderate path loss. The scenario 3, defines a environment with small tree cover; the environment exhibits very minimal path loss. For SUI systems operating in ranges of frequencies beyond 2 GHz, the standard PL calculation is adjusted using the variables mentioned in references [30]-[32]. These variables include the frequency range adjustment X_{fc} and the receiver's height adjustment X_{RX} . The following is the PL_{SUI} in dB is presented using the (11) and (12):

$$PL_{SUI}(d)[dB] = FSPL(f, 1m)[dB] + 10\log_{10}\left(\frac{d}{d_0}\right) + X_{fc} + X_{RX} + X_{\sigma} \tag{11}$$

where,

$$FSPL(1m)[dB] = 20\log_{10}\left(\frac{4}{\delta}\right) + X_{fC} + X_{RX} + X_{\sigma} \tag{12}$$

the variable δ is used to represent the velocity of light in a state of vacuum. The preceding equation is presented in a simplified way, using (13). Also, the variable n is calculated using (14). Further, the variable X_{fC} is evaluated using (15). The computation of the variable X_{RX} for the terrain type A and B is performed using (16). The computation of the variable X_{RX} for the terrain type C is performed according to (17).

$$FSPL(1m)[dB] = 32.4[dB] + 20\log_{10}(f_{GHz}) \tag{13}$$

$$n = a - b \cdot h_{TX}(m) + \frac{c}{h_{TX}(m)} \tag{14}$$

$$X_{fC} = 6\log_{10}\left(\frac{f_{MHz}}{2000}\right), f > 2 \text{ GHz} \tag{15}$$

$$X_{RX} = -10.8\log_{10}\left(\frac{h_{RX}(m)}{2}\right), f > 2 \text{ GHz} \tag{16}$$

$$X_{RX} = -20\log_{10}\left(\frac{h_{RX}(m)}{2}\right), f > 2 \text{ GHz} \tag{17}$$

The variables f_{GHz} , f_{MHz} and f represent the carrier’s frequency in units of GHz , MHz , and Hz , respectively. The value of n denotes the path-loss coefficient. FSPL represents the empty space path-loss in dB at an initial distance of 1 meter. X_{RX} and X_{fC} are modification elements for recipient frequencies and heights, respectively. Lastly, X_{σ} represents a zero-valued mean shadowing parameter having standard deviation of σ .

3.5. Channel gain study

In the context of wireless communication systems, it is observed that the user with the highest channel-gain possesses the capability to successfully decode and recover the signals transmitted by other users who have comparatively lower channel-gains. According to the channel-gain order, it can be observed that the channel-gain values follow the sequence $h_1 > h_2 > h_3 > h_4$. The proposed methodology involves the implementation of a three-level SIC technique in order to mitigate the impact of signals originating from r_2 , r_3 , and r_4 . In the same way, it is worth noting that r_2 will utilize a two-level SIC technique in order to successfully remove the signals from both r_3 and r_4 . On the other hand, r_3 will use a single-level SIC approach to solely remove the signals from r_4 . Lastly, because of its specific characteristics, namely a low channel-gain and significant power, r_4 is going to immediately decode its own signal without any SIC technique. In the context of a multi-user downlink situation, it is observed that powerful users are able to effectively mitigate the interference resulting from weakened users by employing SIC technique. As a result, these powerful users are able to achieve higher levels of throughput in comparison to their weaker counterparts. The (18) denoting the throughput of user r_i within the multi-user downlink PD-NOMA situation can be found in reference [33]. Further, in (18), the variable N_i represents the noise power spectrum density associated with the i^{th} user. The data rate attained in the scenario of a multi-user uplink PD-NOMA can be determined using [33].

$$r_i = \log_2\left(1 + \frac{p_i|h_i|^2}{\sum_{j=1}^{i-1} p_j|h_i|^2 + N_i}\right), \quad \forall = 1,2,3,4,5. \tag{18}$$

$$r_i = \log_2\left(1 + \frac{p_i|h_i|^2}{\sum_{j=1}^4 p_j|h_i|^2 + N_i}\right), \quad \forall = 1,2,3,4,5. \tag{19}$$

The primary distinguishing factor among downlink and uplink PD-NOMA lies in the SIC order. In the context of data transmission, it is observed that throughout the downlink phase, the decoding process prioritizes the farthest or weakened user data. Conversely, during the uplink phase, the decoding process gives priority to the nearby or powerful user data. The primary focus of PD-NOMA remains intact as it employs power level-based signal decoding. In either the downlink and uplink, it is imperative to prioritize the decoding of signals with the most power at every respective receiver. Within the context of the downlink, it has been observed that powerful users are able to acquire transmissions without any interference. This desirable outcome is achieved by effectively eliminating the signals from weakened users by means of

the employment of the SIC technique. During the uplink phase, the signals of weakened users undergo decoding after the interference caused by powerful users is eliminated.

4. RESULTS AND ANALYSIS

This section studies the performance of proposed ERA design over existing MUDRA [18]. The overall work is implemented using C# and MATLAB programming language using SIMITS [34], [35] and NYUSIM [36], [37]. In this work, three different scenarios are considered, the scenario 1, defines a complex path loss due to average-heavy tree density and hilly terrain, the scenario 2, defines a moderate path loss due to heavy vegetation at the terrain and hilly terrain climatic condition, scenario 3, defines a minimal path loss due to small tree density at the terrain. The bit error rate (BER) performance is measured considering different SNR i.e., between -0 dB to 30 dB. The Table 1 discusses the simulation parameter considered for evaluation.

Table 1. Simulation parameter

Parameter		Value		
No. of users		100		
User clustering		2 to 5 user/cluster		
Mobility of user		3 to 7 m/s		
Simulation area		100 m * 100 m		
Minimum distance from BS		10 m		
Terrain type		Scenario 1, scenario 2, and scenario 3		
PFs		0 to 1 (Configured as per (5) and (6))		
Filter used		Root raised cosine filter [21]		
Fading channel model		SUI fading channels [21]		
Phase shift		0, $\frac{\pi}{2}$, π , and $\frac{3\pi}{2}$		
Doppler spread frequency		0.25 to 0.5 Hz		
SNR		0 dB to 30 dB		
Path loss		Computed using (11)		
Properties	Scenario 1	Scenario 2	Scenario 3	
Path delay	[0 14 20]	[0 0.4 0.9]	[0 0.4 0.9]	
Path gain	[0-10-14]	[0-5-10]	[0-12-15]	
Doppler spreads	0.5	0.5	0.25	

4.1. BER performance with different SUI fading scenarios

The section studies the performance achieved using MUDRA and ERA in terms of BER under varied SNR for three different scenarios. The BER performance for varied SNR for scenario 1 is graphically shown in Figure 6. From figure it can be interpreted that the proposed ERA model significantly reduces the BER in comparison with MUDRA. The BER performance for varied SNR for scenario 2 is graphically shown in Figure 7. From figure it can be interpreted that the proposed ERA model significantly reduces the BER in comparison with MUDRA. The BER performance for varied SNR for scenario 3 is graphically shown in Figure 8. From figure it can be interpreted that the proposed ERA model significantly reduces the BER in comparison with MUDRA.

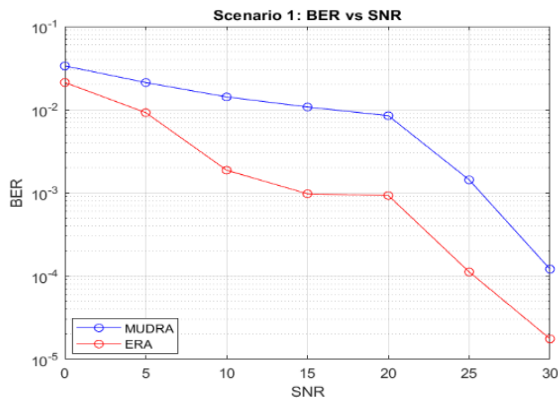


Figure 6. BER performance considering 5 user per cluster for scenario 1

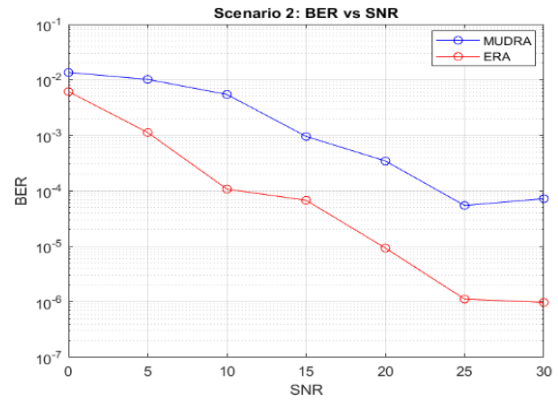


Figure 7. BER performance considering 5 user per cluster for scenario 2

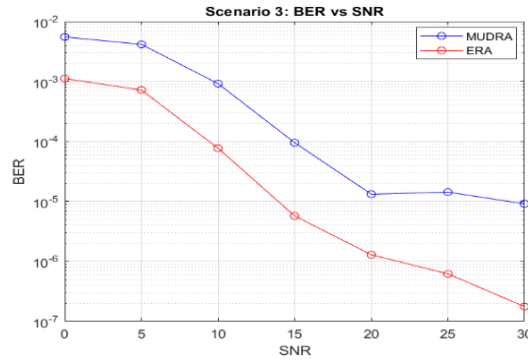


Figure 8. BER performance considering 5 user per cluster for scenario 3

4.2. BER performance with user density per cluster

This section studies the BER performance considering varied user density per cluster where user moves through different environment condition defined in scenarios 1 to 3. The user density is varied from 2 to 5 per cluster and simulation is conducted and BER under varied SNR is graphically described in Figure 9. From figure it can be interpretate as smaller number of users per cluster exhibit less BER and larger number of users per cluster exhibit higher BER.

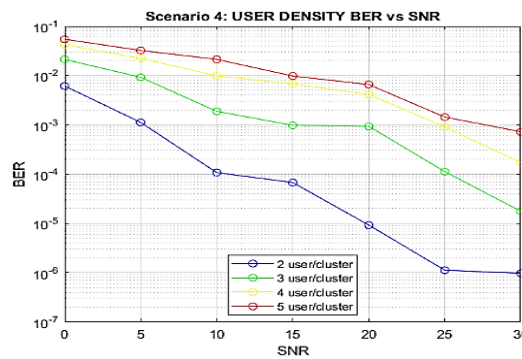


Figure 9. BER performance considering different user density per cluster

4.3. Packet transmission performance

This section studies the throughput performance considering varied user density per cluster and varied mobility speed where user moves through different environment condition defined in scenarios 1 to 3. The user density is varied from 2 to 5 per cluster and simulation is conducted and throughput under varied user per cluster is graphically described in Figure 10. From figure it can be interpretate as smaller number of users per cluster exhibit less throughput and larger number of users per cluster exhibit higher throughput. The user mobility speed is varied between 3 m/s to 7 m/s and simulation is conducted and throughput under varied mobility speed is graphically described in Figure 11. From figure it can be interpretate lesser speed exhibit higher throughput and larger speed exhibit lesser throughput.

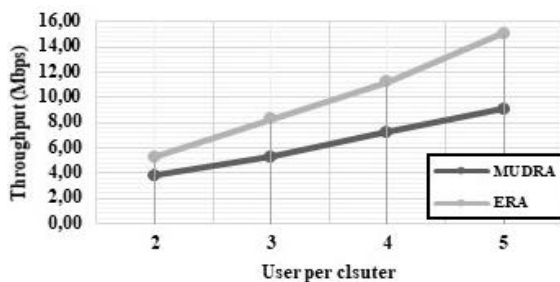


Figure 10. Throughput vs density

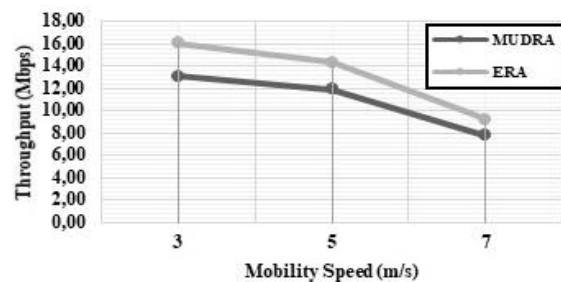


Figure 11. Throughput performance vs mobility speed

5. CONCLUSION

This work introduces an ERA design for PD-NOMA encompassing multiple users. In this work, the model first performs ZC sequence precoding of user's data; then, each user is allocated different power according to its distance (i.e., the signal degraded with increasing in distance between users and BSs). The existing model perform power clustering considering 2 to 4 user per cluster; however, in this work five user per cluster is considered. In further enhancing performance Maximum phase shifts process is added. The performance of ERA is studied in terms of varied SNR considering different scenario using SUI fading model. Total three different scenarios such as heavy, moderate, and small fading is considered. The throughput attained is also studied considering varying speed and number of users per cluster. The result shows increasing number-of user per cluster increases BER in the network; however, higher throughput is experienced when we increase the number of users per cluster, this is because as user are increased more data is generated in the network. the existing resource allocation design in PD-NOMA are tested considering static users; however, in this study the user are mobile in nature; thus, the throughput performance is studied under varied mobility speed. the overall result achieved shows the ERA significantly reduces BER and attain higher throughput in comparison with existing MUDRA model considering SUI fading scenarios. The future work would consider incorporating both LOS and NLOS component in to the propagation model and also incorporate the effect of mobility impacting path-loss in complex urban scenario for effective smart application provisioning.




REFERENCES

- [1] L. Kansal, G. S. Gaba, A. Sharma, G. Dhiman, M. Baz, and M. Masud, "Performance analysis of WOFDM-WiMAX integrating diverse wavelets for 5G applications," *Wireless Communications and Mobile Computing*, vol. 2021, pp. 1–14, Nov. 2021, doi: 10.1155/2021/5835806.
- [2] M. H. Alsharif, A. H. Kelechi, M. A. Albream, S. A. Chaudhry, M. S. Zia, and S. Kim, "Sixth generation (6G) wireless networks: Vision, research activities, challenges and potential solutions," *Symmetry*, vol. 12, no. 4, p. 676, Apr. 2020, doi: 10.3390/sym12040676.
- [3] B. Makki, K. Chitti, A. Behravan, and M.-S. Alouini, "A survey of NOMA: current status and open research challenges," *IEEE Open Journal of the Communications Society*, vol. 1, pp. 179–189, 2020, doi: 10.1109/ojcoms.2020.2969899.
- [4] M. Vaezi, Z. Ding, and H. V. Poor, "Multiple access techniques for 5G wireless networks and beyond," *Cham: Springer International Publishing*, pp. 493-514, 2019, doi: 10.1007/978-3-319-92090-0.
- [5] X. Fu, M. Pischella, and D. L. Ruyet, "Joint uplink PD-NOMA and SCMA for future multiple access systems," *2021 IEEE 93rd Vehicular Technology Conference (VTC2021-Spring)*, Helsinki, 2021, pp. 1-5, doi: 10.1109/VTC2021-Spring51267.2021.9449037.
- [6] Q. Luo *et al.*, "An error rate comparison of power domain non-orthogonal multiple access and sparse code multiple access," *IEEE Open Journal of the Communications Society*, vol. 2, pp. 500-511, 2021, doi: 10.1109/OJCOMS.2021.3064504.
- [7] M. Al-Imrani and M. A. Imran, "Low density spreading multiple access," *Springer eBooks*, pp. 493–514, Aug. 2018, doi: 10.1007/978-3-319-92090-0_15.
- [8] S. Chen, B. Ren, Q. Gao, S. Kang, S. Sun, and K. Niu, "Pattern division multiple access-a novel nonorthogonal multiple access for fifth-generation radio networks," *IEEE Transactions on Vehicular Technology*, vol. 66, no. 4, pp. 3185-3196, April 2017, doi: 10.1109/TVT.2016.2596438.
- [9] E. G. Larsson, O. Edfors, F. Tufvesson, and T. L. Marzetta, "Massive MIMO for next generation wireless systems," *IEEE Communications Magazine*, vol. 52, no. 2, pp. 186-195, February 2014, doi: 10.1109/MCOM.2014.6736761.
- [10] M. Zeng, W. Hao, O. A. Dobre, and Z. Ding, "Cooperative NOMA: state of the art, key techniques, and open challenges," *IEEE Network*, vol. 34, no. 5, pp. 205-211, September/October 2020, doi: 10.1109/MNET.011.1900601.
- [11] A. Mahmood, M. Marey, M. M. Nasralla, M. A. Esmail, and M. Zeeshan, "Optimal power allocation and cooperative relaying under fuzzy inference system (FIS) based downlink PD-NOMA," *Electronics*, vol. 11, no. 9, pp. 1338–1338, Apr. 2022, doi: 10.3390/electronics11091338.
- [12] O. Maraqa, A. S. Rajasekaran, S. Al-Ahmadi, H. Yanikomeroğlu, and S. M. Sait, "A survey of rate-optimal power domain NOMA with enabling technologies of future wireless networks," *IEEE Communications Surveys and Tutorials*, vol. 22, no. 4, pp. 2192-2235, Fourth quarter 2020, doi: 10.1109/COMST.2020.3013514.
- [13] F. Kara and H. Kaya, "BER performances of downlink and uplink NOMA in the presence of SIC errors over fading channels," *IET Communications*, vol. 12, no. 15, pp. 1834–1844, Sep. 2018, doi: 10.1049/iet-com.2018.5278.
- [14] G. Wunder *et al.*, "5GNOW: non-orthogonal, asynchronous waveforms for future mobile applications," *IEEE Communications Magazine*, vol. 52, no. 2, pp. 97-105, February 2014, doi: 10.1109/MCOM.2014.6736749.
- [15] S. Mukhtar and G. R. Begh, "Performance analysis of filtered OFDM based downlink and uplink NOMA system over nakagami-m fading channel," *Journal of Telecommunications and Information Technology*, vol. 2, no. 2021, pp. 11–23, Mar. 2021, doi: 10.26636/jtit.2021.148020.
- [16] S. M. R. Islam, N. Avazov, O. A. Dobre, and K.-S. Kwak, "Power-domain non-orthogonal multiple access (NOMA) in 5G systems: Potentials and challenges," *IEEE Communications Surveys and Tutorials*, vol. 19, no. 2, pp. 721-742, Second quarter 2017, doi: 10.1109/COMST.2016.2621116.
- [17] M. T. P. Le, G. C. Ferrante, G. Caso, L. D. Nardis, and M. D. Benedetto, "On information-theoretic limits of code-domain NOMA for 5G," *IET Communications*, vol. 12, no. 15, pp. 1864–1871, Aug. 2018, doi: 10.1049/iet-com.2018.5241.
- [18] A. Mahmood, S. Khan, S. Hussain, and M. Zeeshan, "Performance analysis of multi-user downlink PD-NOMA under SUI fading channel models," *IEEE Access*, vol. 9, pp. 52851-52859, 2021, doi: 10.1109/ACCESS.2021.3070147.
- [19] E. Sfeir, R. Mitra, and G. Kaddoum, "A random fourier feature based receiver detection for enhanced BER performance in nonlinear PD-NOMA," *IEEE Transactions on Vehicular Technology*, 2022, doi: 10.1109/TVT.2022.3213811.
- [20] R. Parameswaran and P. T. Bhuvaneshwari, "Performance analysis of NOMA under power control mechanism," *2021 Innovations in Power and Advanced Computing Technologies (i-PACT)*, Kuala Lumpur, Malaysia, 2021, pp. 1-5, doi: 10.1109/i-PACT52855.2021.9696636.




- [21] M. Kokilavani, R. K. Siddharth, S. M. Riyaz, P. Ramesh, S. Ezhilarasi, and P. T. V. Bhuvanewari, "Downlink performance analysis of 5G PD-NOMA system," *2022 IEEE Global Conference on Computing, Power and Communication Technologies (GlobConPT)*, Sep. 2022, doi: 10.1109/globconpt57482.2022.9938331.
- [22] T. B. Rejeb, M. G. Bakulin, V. B. Kreyndelin, D. Y. Pankratov, and A. E. Smirnov, "Performance analysis of uplink non-orthogonal multiple access (NOMA)," *2022 Systems of Signals Generating and Processing in the Field of on-Board Communications*, Moscow, Russian Federation, 2022, pp. 1-5, doi: 10.1109/IEEECONF53456.2022.9744088.
- [23] P. N. Thakre and S. B. Pokle, "A survey on power allocation in PD-NOMA for 5G wireless communication systems," *2022 10th International Conference on Emerging Trends in Engineering and Technology - Signal and Information Processing (ICETET-SIP-22)*, Nagpur, India, 2022, pp. 1-5, doi: 10.1109/ICETET-SIP-2254415.2022.9791576.
- [24] S.-M. Tseng and W.-Y. Chen, "Cross-layer codebook allocation for uplink SCMA and PDNOMA-SCMA video transmission systems and a deep learning-based approach," *IEEE Systems Journal*, 2022, doi: 10.1109/JSYST.2022.3168851.
- [25] A. Mahmood, M. Marey, M. M. Nasralla, M. A. Esmail, and H. Mostafa, "Secure PD-NOMA with multi-user cooperation and user clustering in both uplink and downlink PD-NOMA," *Electronics*, vol. 11, no. 14, p. 2153, Jul. 2022, doi: 10.3390/electronics11142153.
- [26] X. Yue, Y. Liu, Y. Yao, X. Li, R. Liu, and A. Nallanathan, "Secure communications in a unified non-orthogonal multiple access framework," *IEEE Transactions on Wireless Communications*, vol. 19, no. 3, pp. 2163-2178, 2020, doi: 10.1109/TWC.2019.2963181.
- [27] A. Mahmood and M. Zeeshan, "Power allocation and performance analysis of multiuser NOMA under NYUSIM channel model," *2019 14th Conference on Industrial and Information Systems (ICIIS)*, Kandy, Sri Lanka, 2019, pp. 296-301, doi: 10.1109/ICIIS47346.2019.9063340.
- [28] T. Kaitz and B. Trinkwon, "Title channel models for fixed wireless applications date," 2001, Accessed: Dec. 03, 2023. [Online]. Available: https://www.ieee802.org/16/tg3/contrib/802163c-01_29r4.pdf.
- [29] V. Erceg et al., "An empirically based path loss model for wireless channels in suburban environments," *IEEE Journal on Selected Areas in Communications*, vol. 17, no. 7, pp. 1205-1211, July 1999, doi: 10.1109/49.778178.
- [30] A. I. Sulyman, A. Alwarafy, G. R. MacCartney, T. S. Rappaport, and A. Alsanie, "Directional radio propagation path loss models for millimeter-wave wireless networks in the 28-, 60-, and 73-GHz bands," *IEEE Transactions on Wireless Communications*, vol. 15, no. 10, pp. 6939-6947, Oct. 2016, doi: 10.1109/TWC.2016.2594067.
- [31] A. I. Sulyman, A. T. Nassar, M. K. Samimi, G. R. Maccartney, T. S. Rappaport, and A. Alsanie, "Radio propagation path loss models for 5G cellular networks in the 28 GHz and 38 GHz millimeter-wave bands," *IEEE Communications Magazine*, vol. 52, no. 9, pp. 78-86, September 2014, doi: 10.1109/MCOM.2014.6894456.
- [32] P. D. Katev, "Propagation models for WiMAX at 3.5 GHz," *2012 ELEKTRO*, Rajecke Teplice, Slovakia, 2012, pp. 61-65, doi: 10.1109/ELEKTRO.2012.6225572.
- [33] S. M. R. Islam, M. Zeng, O. A. Dobre, and K.-S. Kwak, "Non-orthogonal multiple access (NOMA): how it meets 5G and beyond," *arxiv.org*, Jul. 2019, doi: 10.48550/arXiv.1907.10001.
- [34] M. Manzano, F. Espinosa, Á. M. Bravo-Santos, and A. Gardel-Vicente, "Cognitive self-scheduled mechanism for access control in noisy vehicular Ad Hoc networks," *Hindawi*, vol. 2015, pp. 1-12, Jun. 2015, doi: 10.1155/2015/354292.
- [35] Al-Absi, Al-Absi, and J. Lee, "Performance enriching channel allocation algorithm for vehicle-to-vehicle city, highway and rural network," *Sensors*, vol. 19, no. 15, p. 3283, Jul. 2019, doi: 10.3390/s19153283.
- [36] S. Sun, G. R. MacCartney, and T. S. Rappaport, "A novel millimeter-wave channel simulator and applications for 5G wireless communications," *2017 IEEE International Conference on Communications (ICC)*, Paris, France, 2017, pp. 1-7, doi: 10.1109/ICC.2017.7996792.
- [37] S. Ju, O. Kanhere, Y. Xing, and T. S. Rappaport, "A millimeter-wave channel simulator NYUSIM with spatial consistency and human blockage," *2019 IEEE Global Communications Conference (GLOBECOM)*, Waikoloa, HI, USA, 2019, pp. 1-6, doi: 10.1109/GLOBECOM38437.2019.9013273.

BIOGRAPHIES OF AUTHORS



Vanita Kaba    working assistant professor at Sharnbasva University Kalaburagi. Obtained a Bachelor of Engineering degree in Electronics and Communication Engineering from Pooja Doddappa Appa Engineering College Kalaburagi in 2007, Master of Technology in Digital Electronics and Communication from DayandaSagar College of Engineering Bangalore, Karnataka, India, in 2013 and pursuing a Ph.D. Publications: Two International conferences and one International Journal. Member of IEEE and Member of IETE, IAENG. She can be contacted at email: vbkaba@gmail.com.



Dr. Rajendra R. Patil    received Bachelor of Engineering in Electronics and Communication Engg, PDAEC, Kalaburagi in 1991, Master of Technology in Power Electronics, PDAEC, Kalaburagi in 2006 and Ph.D. in Applied Electronics (Microwave), Gulbarga University, Kalaburagi in 2016. He is working as Professor and HOD at GSSS IET for Women, Mysuru, India. Inventor for 2-patents, filed in Aug. 2019 and Feb. 2020 in the areas of VLSI and computerized vehicle control. Senior Member of IEEE and Member of ISTE, IAENG. His main research interests are microwave engineering, wireless communication, and embedded systems. He can be contacted at email: rajendra.nano@gmail.com.